

TECHNICAL SCIENCES

Abbrev.: Techn. Sc., No 13, Y 2010

DOI 10.2478/v10022-010-0025-4

THE COMPUTER ANALYSIS SHAPE OF REFLEXES XRD ON THE BASIS OF X2CrNiMoN25-7-4 STEEL

Paweł Szabracki, Miroslaw Bramowicz, Tomasz Lipiński

Department of Materials and Machines Technology
University of Warmia and Mazury in Olsztyn,

K e y w o r d s: XRD diffractometry, XRD, Pearson VII, Gauss, Cauchy.

A b s t r a c t

This paper was introduced the author's program to the analysis of the shape of XRD reflexes. The analysis was subjected results fittings of numerical models to data got during measurements. The method of the smallest squares of mistakes was used in the analysis of the fitting. The written application lets describe peak using one from popular functions. Parameters of the diffractive reflex appointed with the program let determine lattice parameters, volumetric phase participation and determine the quantity of crystallites and network distortions.

KOMPUTEROWA ANALIZA KSZTAŁTU REFLEKSÓW XRD NA PRZYKŁADZIE STALI X2CrNiMoN25-7-4

Paweł Szabracki, Miroslaw Bramowicz, Tomasz Lipiński

Katedra Technologii Materiałów i Maszyn
Uniwersytet Warmińsko-Mazurski w Olsztynie

S l o w a k l u c z o w e: dyfrakcja rentgenowska, XRD, Pearson VII, Gauss, Cauchy.

A b s t r a c t

W artykule przedstawiono autorski program do analizy kształtu refleksów XRD. Przeanalizowano wyniki dopasowania modeli numerycznych do wyników uzyskanych podczas pomiarów rzeczywistych. W analizie dopasowania wykorzystano metodę najmniejszych kwadratów błędów. Aplikacja pozwoliła opisać pik za pomocą jednej z dostępnych funkcji. Wyznaczone za pomocą programu parametry refleksu dyfrakcyjnego pozwalają na określenie parametrów sieciowych, objętościowych udziałów fazowych oraz wyznaczenie wielkości krystalitów i zniekształceń sieciowych.

Introduction

X-ray diffractometry (XRD – eng: X-Ray Diffraction) delivers a lot of valuable information about the structure and properties of materials. She lets e.g.: the precise measurement of lattice parameters, determining phase participation, determine of the size of crystallites and the measurement of stresses and network deformation. The result of XRD measurements are registered as dependencies of the intensity of the bent X-ray bundle, subjected to the right according Bragg law of diffraction on the atoms of the crystalline lattice, in the function of the angle of deflection (2Θ), so-called diffraction patterns (BOJARSKI, ŁĄGIEWKA 1988, BOJARSKI, BOŁD 1970, CULLITY 1964, OLESZAK, OLSZYNA 2004, SENCZYK 1995).

In the present work analyzed the influence of the shape of the diffractive peak profile circumscribed the functions: Gauss, Cauchy and Pearson VII, on their basic parameters, such as: the location of the centre of gravity, total and integral intensity, half-value width.

In this aim it was created in the Delphi the application designed to the numeric analysis diffraction patterns whose working was proved on example registered diffraction pattern (Fig. 1) the sample of steel X2CrNiMoN25-7-4 submitted earlier annealing in temp. 1100°C for 30 min., and then saturated in water to the temperature of surroundings.

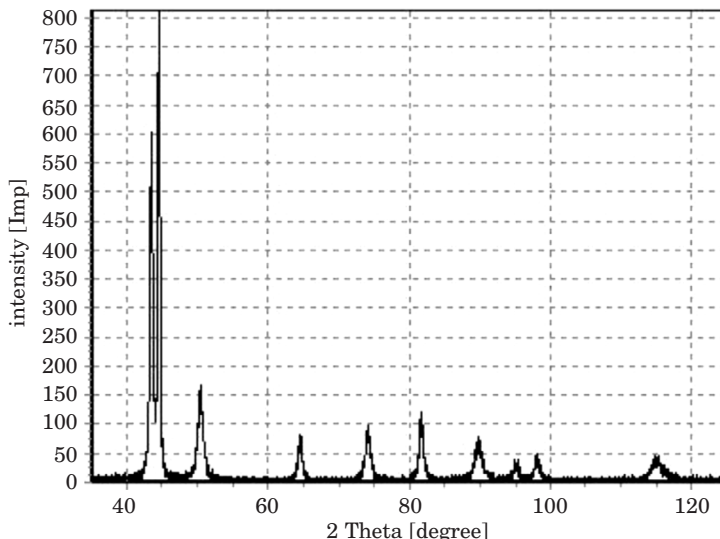


Fig. 1. Diffraction pattern of X2CrNiMoN25-7-4 steel after annealing 30 minutes at temperature 1100°C, cooling in water

The measurements were conducted on the diffractometer X-ray X'Pert PRO with focusing according to Bragg-Brentano and the prostate registration of impulses. in investigations applied radiance of characteristic CuK_α about the weighted average of the length of the wave $\lambda = 1,541783$. The measurements were conducted in range of angle 2Θ from 35 to 125° , value power of the measuring step carried out 0.02° , meanwhile time of counting impulses 2 sec.

Parameters characterizing the profile of the diffraction line

Every diffraction reflex is characterized a few of the parameters to which belongs the location of the diffraction line, total intensity the half-value and integral width. These quantities can be assigned on the basis of function circumscribing the profile of the diffraction line (BOJARSKI, ŁĄGIEWKA 1988, CULLITY 1964, SENCZYK 1995).

The gauge of the total intensity of the diffraction line is the surface bounded curve expansion of intensity in the diffraction line and the line of the background taken by horizontal intervals the side branches of the diffraction line. It is defined as (BOJARSKI, ŁĄGIEWKA 1988, CULLITY 1964, SENCZYK 1995):

$$I_c = \int_{\Theta_1}^{\Theta_2} I(\Theta) d(\Theta) \quad (1)$$

where:

$I(\Theta)$ – the function of the expansion of the intensity of the diffraction line,
 Θ_1, Θ_2 – points, where diffraction line is equal to background.

The half-value width $\beta_{1/2}$ of diffraction line according to Sherrer is defined as width of the reflex in the half of his maximum intensity (BOJARSKI, ŁĄGIEWKA 1988, CULLITY 1964, SENCZYK 1995).

The integral width (2) according to Maxa von Laue is defined as quotient of total intensity of the diffraction line to maximum intensity (SENCZYK 1995):

$$\beta_c = \frac{I_c}{I_{\max}} \quad (2)$$

where:

I_c – total intensity of the diffraction line (1),

I_{\max} – maximum intensity of diffraction line.

The position of the diffraction line is defined as position of top or the centre of gravity of the diffraction line. Assignment of the position of the top is easier to the execution, but less exact and shouldn't be applied to the precise measurements of the crystalline lattice or the measurements of stress. Defining the position of the diffraction line through the assignment of the the centre of gravity of the analyzed reflex is recommended to exact analysis.

Necessary diffraction pattern is not in the analysis of got results, as the integer, but position and sizes characterizing individual reflexes. SENCZYK (1995) gives the equations of functions used to the description of the expansion of the intensity of the diffraction line. As first, author exchanges circumscribed the formula (3) Gauss function (BOJARSKI, ŁĄGIEWKA 1988, CULLITY 1964, SENCZYK 1995):

$$I(x) = I_0 e^{-kx^2} \quad (3)$$

where:

I_0 – intensity in top of function,

k – coefficient circumscribing course of the function.

The coefficients I_0 and k has influence on the shape of the function Gauss. Established maximum intensity $I_0 = 0,8$ for all analyzed models will let eliminate the changes the function shape resulting from the change of this value. The solid values of coefficients circumscribing the background ($y(x) = ax + b$, where $a = 0, b = 0,05$) were accepted in the aim of the qualification of the homogeneous conditions of the analysis of the results of investigations. The influence of the change of the coefficient value on the course of the Gauss function was introduced at Fig. 2.

As follow from Fig. 2. together with the growth of the k coefficient value, the shape of profile Gauss function changes. Profile this becomes narrower more and more and simultaneously the radius of the profile curvature diminishes at the basis. The radius of curvature in the top of the function diminishes together with the growth of the k coefficient value. Growth of the value of the analyzed parameter causes faster achievement by the profile of the function level of the background.

Following described by Senczyk function is Cauchy (BOJARSKI, ŁĄGIEWKA 1988, CULLITY 1964, SENCZYK 1995) function described by formula (4):

$$I(x) = I_0 \frac{1}{1 + kx^2} \quad (4)$$

where:

I_0 – intensity in top of function,

k – coefficient circumscribing course of the function.

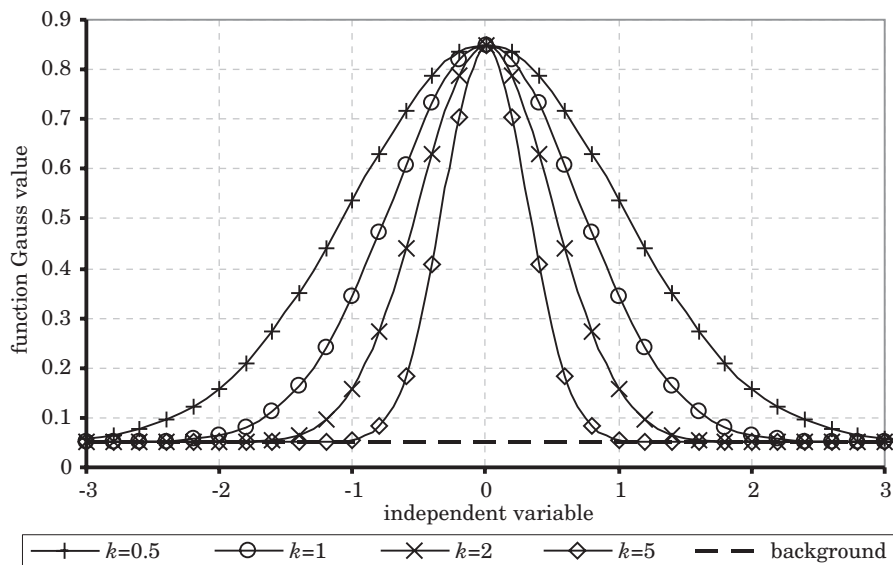


Fig. 2. The expansion of Gauss function in dependence from the value of the coefficient k

Graphic interpretation of influence of coefficient k value change (Fig. 3) was created in the aim of the view the influence parameters of model on the shape of the curve circumscribed by model Cauchy (4) on the course of the function Cauchy.

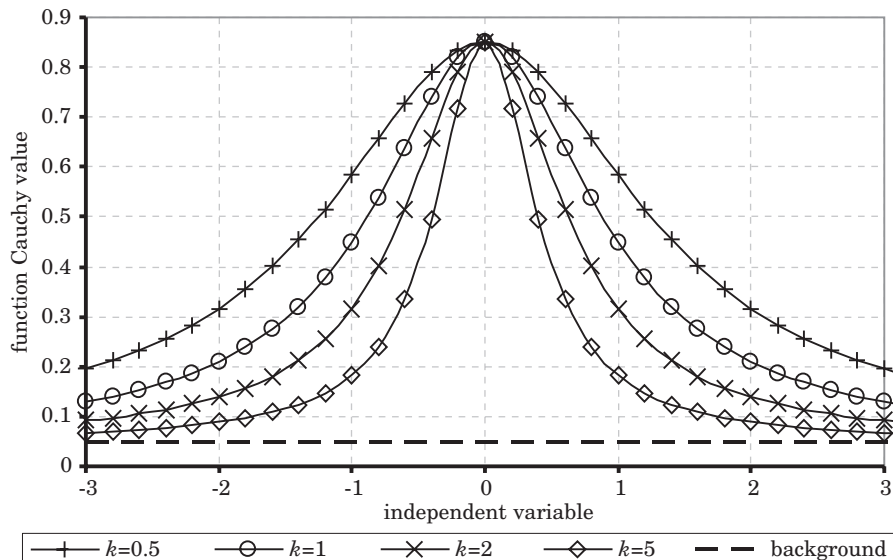


Fig. 3. The expansion of Cauchy function in dependence from the value of the coefficient k

The course of the Cauchy (Fig. 3) function differs from course of function Gauss considerably. Considerably larger radius of the curvature of the function profile near basis (passage to the value of the background) visible is than in case of Gauss function (Fig. 2). The profile of the function is also considerably wider on these same values of the coefficient k . Similarly as the Gauss, radius of the profile curvature the function near the top grows together with the fall of the value of the coefficient k . Profile of the function Cauchy brings nearer more considerably slowly oneself to the background.

Another, used in practice function to describe diffraction peaks is function Pearson VII (BOJARSKI, ŁĄGIEWKA 1988, CULLITY 1964, SENCZYK 1995) described by formula (5):

$$I(x) = I_0 \left[1 + \frac{x^2}{ma^2} \right] \quad (5)$$

where:

I_0 – intensity in top of function,

m, a – coefficients circumscribing course of the function.

In aim of qualification of influence coefficients m, a of equation (5) on course of function (5) was analyzed separately influence every one of coefficients from on the foundation of the solid value the not analyzed at the moment coefficient. Influence of coefficient m value change on course of function (5) was introduced on the solid value of the coefficient $a = 0.5$ at Fig. 4.

The growth of the value of coefficient m causes decrease of the radius of curvature of the profile Pearson VII (5) at the basis (near passage to the level of the background Fig. 4). The growth of the value of the coefficient m causes quicker simultaneously you will reach the value of the background by the profile. Obtainment of the smaller half-value width of the profile of the function is the effect of this. In the distinction from circumscribed earlier situations, when one parameter and changed profile of the function both at the basis as and in the top, parameter m of the function Pearson VII (5) influences only the profile of the function at the basis, that is the dynamics of achieving the level of the background.

Next case analyzed according to formula (5), then the influence of the change of the value of the coefficient a (5). The influence of the change of the power of the coefficient a was introduced at fig. 5. on course of function Pearson VII (5) on the constant value of the coefficient $m = 1$.

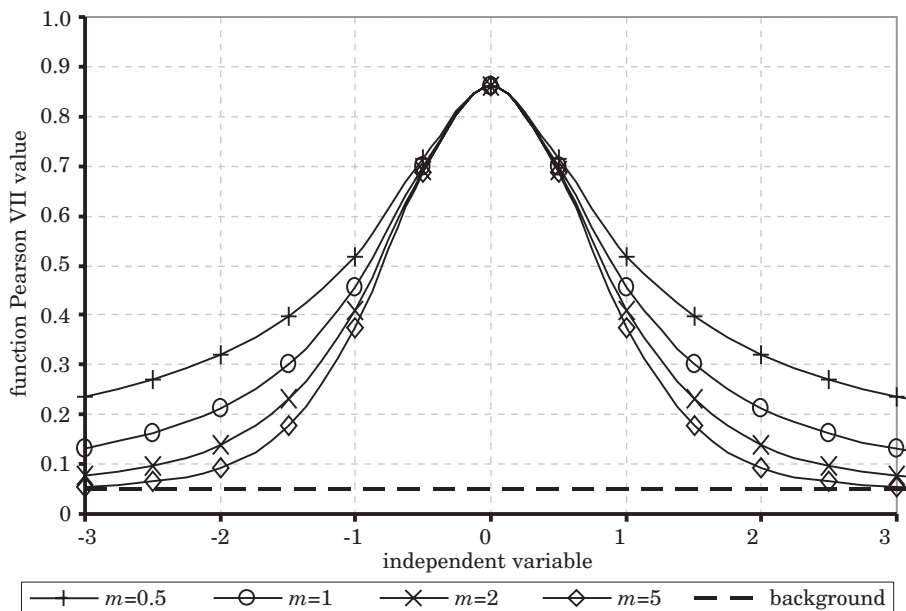


Fig. 4. The expansion of Pearson VII function in dependence from the value of the coefficient m for $a = 0.5$

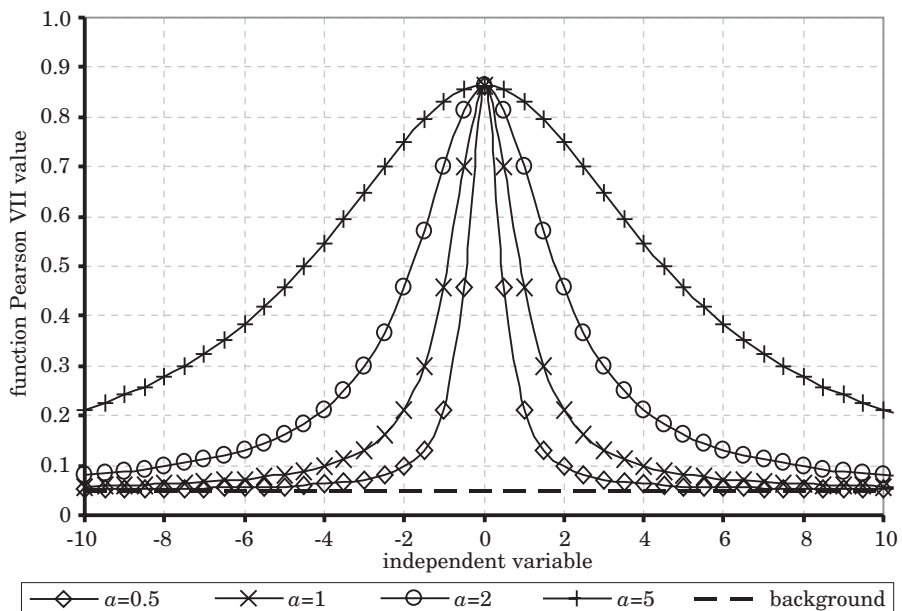


Fig. 5. The expansion of Pearson VII function in dependence from the value of the coefficient a for $m = 1$

The change of the parameter a of Pearson VII function (5) causes the change of the profile in top of function (Fig. 5). But growth of the value of the coefficient a is causes enlargement of the radius of the curve of the section of the function in the top. This change also attracts for her the change of the radius of the curvature of profile in the bottom part of the profile obviously. The bottom part of profile we can additionally control by the coefficient m of equation Pearson VII.

Composition of cases analyzed at Fig.4 and Fig.5 was introduced at Fig. 6 in the aim of demonstrating of considered situations. The composition profiles of the function Pearson VII (5) was introduced at Fig. 6. for the combination of coefficients $a = 0,5$, $a = 1$ and $m = 0,5$, $m = 2$. He results from them, that after the change of the coefficient a , the bottom parts of the profile of function for constant value of the coefficient m are not parallel in relation to themselves (the lines $a = 0,5$, $m = 2$ and $a = 1$, $m = 2$).

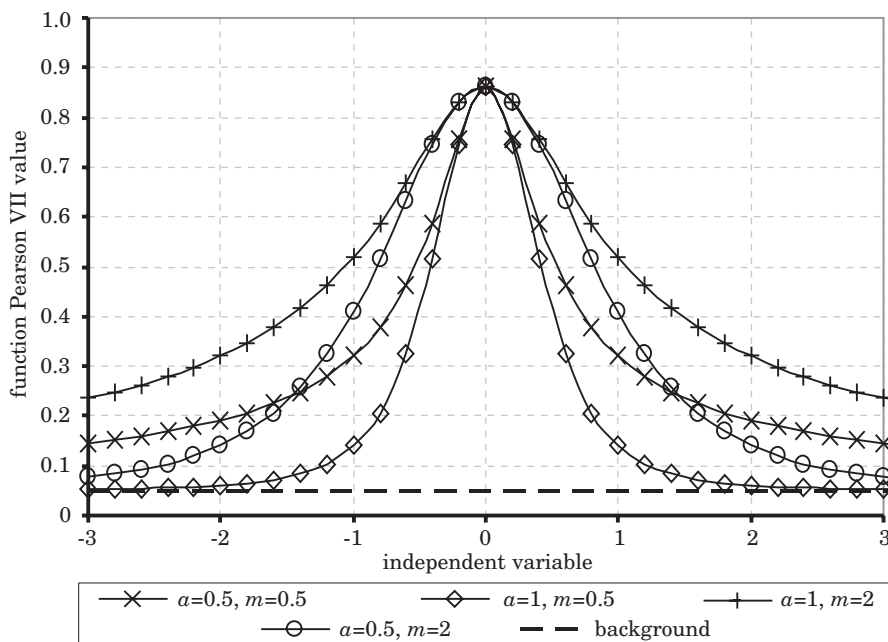


Fig. 6. Expansion of the function Pearson VII for $a = 0,5$, $a = 1$ and $m = 0,5$, $m = 2$

Because of this fits the coefficients of mathematical model to measuring data should complex be held.

In the aim of the efficient analysis of reflexes, computer program enabling obtainment of the parameters of diffraction lines in easy way and first of all quick was created. The program fits mathematical model to experimental data

with utilization of the method of the smallest squares of mistakes according to formula (6).

$$B = \sum_{\Theta_1}^{\Theta_2} [(I(\Theta) - F(\Theta))^2] \quad (6)$$

where:

$I(\Theta)$ – intensity measured for Θ angle,

$F(\Theta)$ – intensity calculated for Θ angle,

$(\Theta)_1, (\Theta)_2$ – range of angles Θ .

The correctness of the work of the individual moduluses of program and application as integral was verified with utilization of different accessible tools enabling the homothetic analysis (Mathcad) and through the analysis standard, circumscribed data. The sequence of moduluses being responsible for delimitation of individual parameters was created on the basis of the analysis of parameters circumscribing diffraction reflexes. As the determinant of the adjustment experimental data to mathematical model coefficient of line correlation (IGNATCZYK, CHROMIŃSKA 1999, TAYLOR 1999) was used:

$$r_{xy} = \frac{\text{cov}(xy)}{\sigma_x \sigma_y} \quad (7)$$

where:

$$\sigma_x = \sqrt{\frac{\sum_{i=1}^n (x_i - \bar{x})^2}{n}} \quad (8)$$

$$\sigma_y = \sqrt{\frac{\sum_{i=1}^n (y_i - \bar{y})^2}{n}} \quad (9)$$

Figure 7 introduced informative card of created application. Program wrote in Delphi 7 Personal (BORLAND SOFTWARE CORPORATION) and he can be used for non commercial usage.

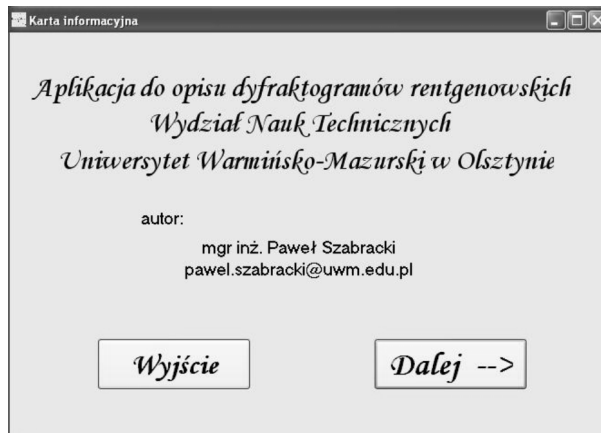


Fig. 7. The informative card of created program

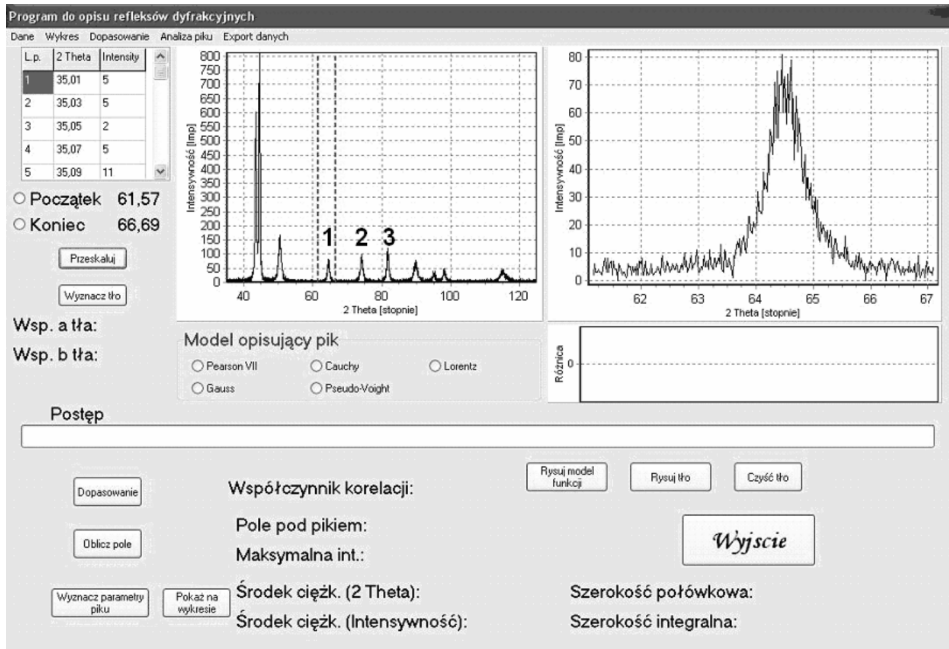


Fig. 8. Program interface

The interface of the application was introduced at Fig. 8 after reads diffraction pattern (left graph) and scaling analyses peak (right upper graph). The mark analysis peak is holds through clicking on the read diffraction pattern of points defining beginning and the end of analyzed reflex near

suitable choice fields of type radio-button for beginning and the end of the range. The right graph representing is enlarged the analyzed reflex about 20 measuring points before the indicated point as beginning and 20 measuring points behind the final point. Mine this on the aim qualification of adjustment of background and function circumscribing beyond the borders of the analyzed range. Additional points on beginning and the end of the range are not taken under the attention near guided calculations.

The comparison of models circumscribing diffraction reflexes

In the aim of proving the correctness of the rule the created application, the qualification the grade adjustment of individual curves to experimental data and proving the influence of the choice of function circumscribing the shape of the reflex on his basic parameters remembered in pkt.1 was used diffraction pattern of the sample X2CrNiMoN25-7-4 steel after the thermal processing. Three (marked at Fig. 8) were chose to the more far analysis the peaks whose profile were circumscribed individual functions. Adjustment of model Gauss (3) to analysis peak was introduced at Fig. 9.

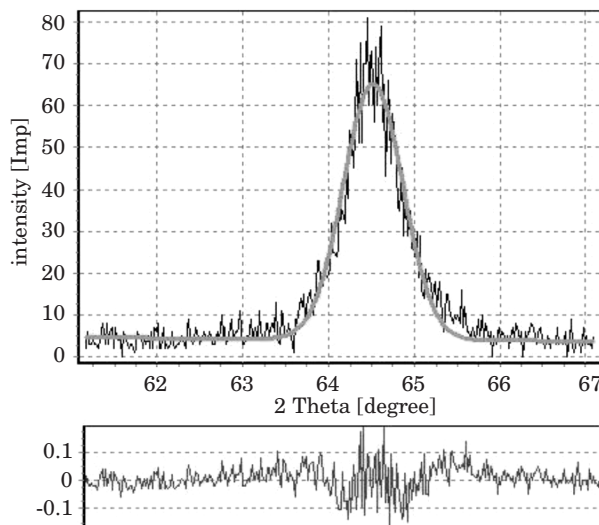


Fig. 9. Fitting Gauss model (3) to experimental data

Figure 10 introduced graphical fitting Cauchy model (4) to the same range of experimental data as for Gauss model (3).

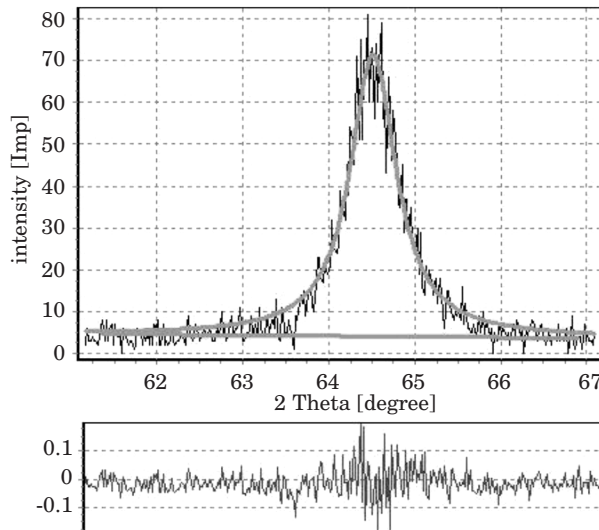


Fig. 10. Fitting Cauchy model (4) to experimental data

Figure 10 except the fitting of mathematical model, the graphic introduction of the background which is marked to consider in the calculations of the individual parameters of the reflex was also introduced.

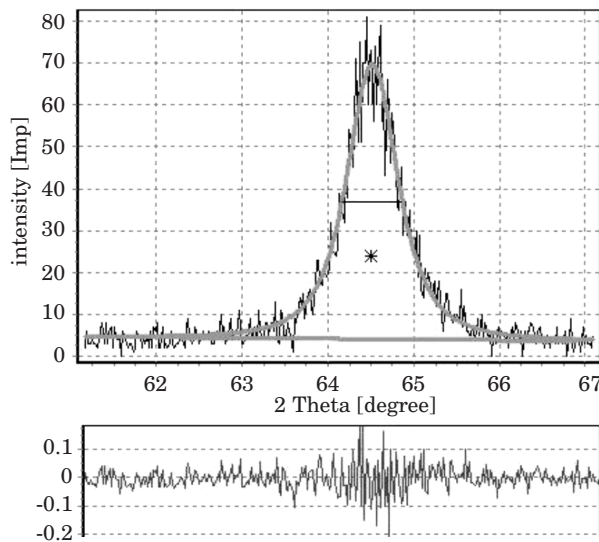


Fig. 11. Fitting Pearson VII model (5) to experimental data

The adjustment of Pearson VII model (5) was introduced graphical at Fig. 11. to experimental data. The position of the the centre of gravity (star) and line defining position and size of the half-value width $\beta_{1/2}$ were introduced graphical additionally. The analysis of the adjustment of above mentioned models was conducted for the uniform values of coefficients circumscribing the background. In table 1 was introduced the composition of parameters characterizes the reflex no. 1 appointed at Fig. 8, appointed using exchanged mathematical models.

Table 1
The comparison of circumscribing parameters the diffraction reflex (no. 1 at Fig. 8) from analyzed diffraction pattern

Specification	Model Gauss	Model Cauchy	Model Pearson VII
Total intensity	53.09	63.39	58.60
Max. intensity	61.13	67.30	65.67
Centre of gravity (2Θ)	64.52	64.474	64.507
Half-value width $\beta_{1/2}$	0.82	0.660	0.7
Integral width β_c	0.868	0.942	0.892
Correlation coefficient	0.971	0.976	0.977
Range of angles (2Θ)	61.57 – 66.69		
Function of background	$f(2\Theta) = 0.01458 \cdot 2\Theta + 4.1067$		

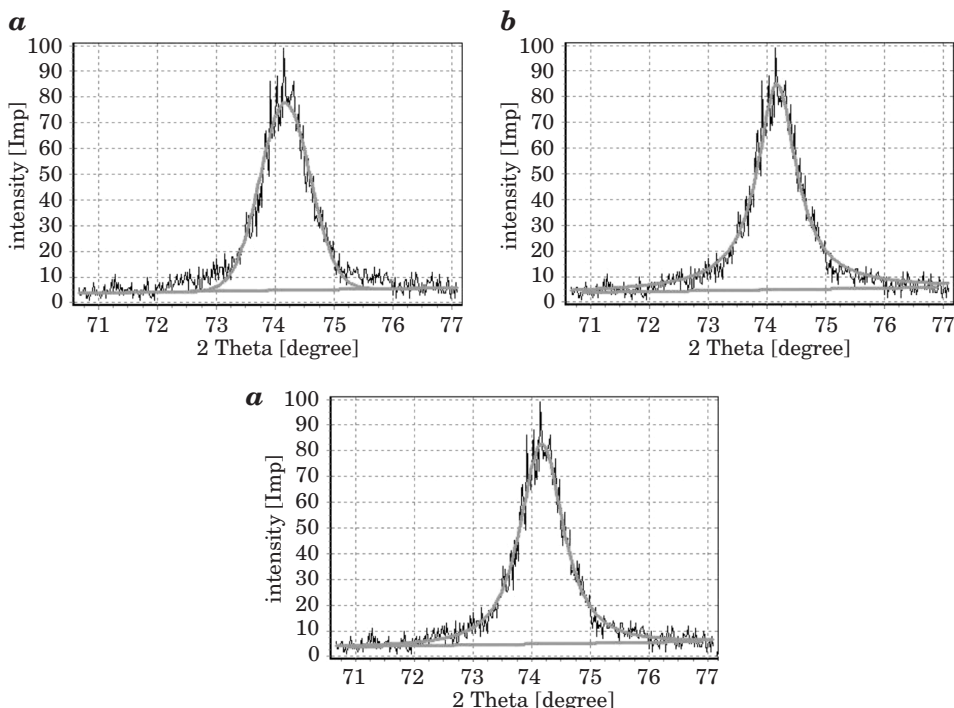


Fig. 12. Fitting models: Gauss (a), Cauchy (b), Pearson VII (c) to experimental data (peak 2 fig. 8)

Fitting of mathematical models: Gauss (*a*) Cauchy (*b*) and Pearson VII (*c*) to experimental data describing peak 2 (Fig. 8.) introduced at Fig. 12. Values of coefficients describing this peak compared in table 2.

Table 2
The comparison of circumscribing parameters the diffraction reflex (no. 2 at Fig. 8) from analyzed diffraction pattern

Specification	Model Gauss	Model Cauchy	Model Pearson VII
Total intensity	77.95	92.39	87.45
Max. intensity	72.76	79.99	77.71
Centre of gravity (2Θ)	74.173	74.1354	74.160
Half-value width $\beta_{1/2}$	1	0.8	0.880
Integral width β_c	1.071	1.155	1.125
Correlation coefficient	0.978	0.98	0.982
Range of angles (2Θ)		71.07 – 76.69	
Function of background		$f(2\Theta) = 0.3267 \cdot 2\Theta + 4.8609$	

Fitting of mathematical models: Gauss (*a*), Cauchy (*b*) and Pearson VII (*c*) to experimental data describing peak 3 (Fig. 8.) introduced at Fig. 13.

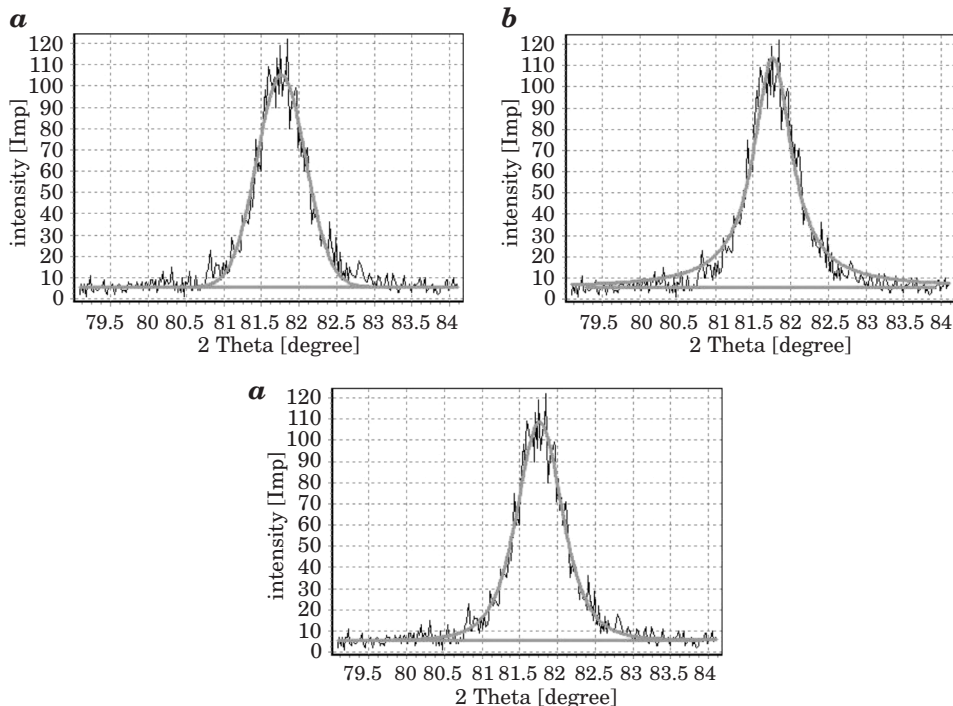


Fig. 13. Fitting models: Gauss (*a*), Cauchy (*b*), Pearson VII (*c*) to experimental data (peak 3 Fig. 8)

Graphical interpretation of fitting numerical models to experimental data introduced on fig. 13. Values of coefficients describing peak 3 (Fig. 8) introduced in table 3.

Table 3
The comparison of circumscribing parameters the diffraction reflex (no. 3 at Fig. 8) from analyzed diffraction pattern

Specification	Model Gauss	Model Cauchy	Model Pearson VII
Total intensity	80.50	95.03	85.74
Max. intensity	99.54	108.1	103.18
Centre of gravity (2Θ)	81.765	81.736	81.762
Half-value width $\beta_{1/2}$	0.76	0.62	0.7
Integral width β_c	0.809	0.879	0.831
Correlation coefficient	0.983	0.98	0.984
Range of angles (2Θ)	79.49 – 83.71		
Function of background	$f(2\Theta) = 0.0488 \cdot 2\Theta + 5.49$		

Summary

Applied in the program mathematical models are applied functions to the description of diffraction reflexes the most often. Each of them lets circumscribe the profile peak with the various grade of the adjustment. which the coefficient of the correlation characterizes.

Function Pearson VII (5) gives the best adjustment of model to experimental data (the highest value of the coefficient of the line correlation). This is caused the independent description of the individual fragments of the curve by the successive parameters of the equation.

The got high values of the coefficients of correlation for individual mathematical models circumscribing the profile of the diffraction line testify about the built correctly algorithm of the program and confirm his usefulness in the numeric analysis of results got by methods XRD. The appointed for the help of the program parameters of the diffractive reflex allow to the qualification of the parameters of lattice structure. volumetric phase participation and marking the size of crystallites and network deformation by the methods: Gauss-Gauss. Cauchy-Gauss. Cauchy-Cauchy (BOJARSKI, BOŁD 1970, OLESZAK, OLSZYNA 2004).

References

- BOJARSKI Z., ŁĄGIEWKA E. 1988. *Rentgenowska analiza strukturalna*. Państwowe Wydawnictwa Naukowe, Warszawa.
- BOJARSKI Z., BOŁD T. 1970. *Rentgenograficzne metody wyznaczania wielkości zniekształceń sieciowych i wielkości bloków materiałów polikrystalicznych*. Prace Instytutów Hutniczych, 3: 115.
- BORLAND SOFTWARE CORPORATION. Licencja produktu Borland Delphi 7 Personal.Cullity B.D. 1964. Podstawy dyfrakcji promieni rentgenowskich. Państwowe Wydawnictwa Naukowe, Warszawa. http://www.borland.pl/licencje_produkty/Delphi_7_Personal_licencja_pl.pdf
- IGNATCZYK W., CHROMIŃSKA M. 1999. *Statystyka teoria i zastosowanie*. Wydawnictwo Wyższej Szkoły Bankowej, Poznań.
- OLESZAK D., OLSZYNA A. 2004. *Określanie wielkości krystalitów i odształceń sieciowych w nanokompozycie NiAl-Al₂O₃ na podstawie poszerzenia rentgenowskich linii dyfrakcyjnych*. KOMPOZYTY (COMPOSITES), 4: 11.
- SENCZYK D. 1995. *Dyfraktometria rentgenowska w badaniach stanów naprężenia i własności sprężystych materiałów polikrystalicznych*. Wydawnictwo Politechniki Poznańskiej. Poznań.
- TAYLOR J.R. 1999. *Wstęp do analizy błędu pomiarowego*. Państwowe Wydawnictwa Naukowe, Warszawa.